

## Preliminary evaluation of $\text{NaClO}_2$ powder injection method for mercury oxidation: Bench scale experiment using iron-ore sintering flue gas

Youngchul Byun, Kiman Lee, Jeonghyun Kim, Dong Jun Koh, and Dong Nam Shin<sup>†</sup>

Environmental Research Department, Research Institute of Industrial Science and Technology,  
Hyoja Dong, Pohang, Gyeongbuk 790-600, Korea  
(Received 5 April 2010 • accepted 15 September 2010)

**Abstract**—The injection of powdered sodium chlorite ( $\text{NaClO}_2(s)$ ) for mercury oxidation into iron-ore sintering flue gas has been evaluated by using the bench scale of tubular flow reactor, where the flow rate and temperature of flue gas stream were controlled to  $250 \text{ Nm}^3 \text{ hr}^{-1}$  and  $135^\circ\text{C}$ , respectively, and either 50 or  $260 \mu\text{g Nm}^{-3}$  of the mercury concentration was introduced intentionally to the gas stream. We have observed that 90% of  $\text{Hg}^0$  oxidation was obtained at  $0.18 \text{ g Nm}^{-3}$   $\text{NaClO}_2(s)$  injection, indicating that the oxidized weight of  $\text{Hg}^0$  by the loaded weight of  $\text{NaClO}_2(s)$  is  $1026 (\pm 333) (\mu\text{g-Hg}^0) (\text{g-NaClO}_2(s))^{-1}$ . This result leads us to suggest that the simple injection of  $\text{NaClO}_2(s)$  into the flue gas has the potential to achieve over 90% mercury control in practical application.

Key words: Sodium Chlorite, Mercury, Oxidation, Real Plant, ClO

### INTRODUCTION

Mercury, as a highly toxic pollutant, tends to be bio-accumulate in the food chain with adverse effects on human health [1,2]. A large portion of anthropogenic mercury emissions comes from municipal waste combustors and coal-burning utilities [1]. Mercury emissions occur in association with particulate matter ( $\text{Hg}^0$ ), gaseous elemental form ( $\text{Hg}^0$ ), and various gaseous mercuric compounds ( $\text{Hg}^{2+}$ ) [1]. Although  $\text{Hg}^{2+}$  and  $\text{Hg}^0$  can be effectively removed by conventional air pollution control devices such as electrostatic precipitation (ESP) and flue gas desulfurization (FGD),  $\text{Hg}^0$  is harder to capture because of its high vapor pressure and low water solubility. Unfortunately, the vast majority of mercury is emitted in the form of  $\text{Hg}^0$ . Therefore, most studies are focused on the oxidation of  $\text{Hg}^0$  to  $\text{Hg}^{2+}$  species, such as  $\text{HgO}$  and  $\text{HgCl}_2$ , for the effective control of mercury emission.

In our previous studies, we examined the oxidation of NO by using powdered sodium chlorite ( $\text{NaClO}_2(s)$ ) in laboratory scale. It was found that NO oxidizes to  $\text{NO}_2$  by  $\text{NaClO}_2(s)$  and in turn  $\text{NO}_2$  reacts with  $\text{NaClO}_2(s)$  leading to the formation of  $\text{OCIO}$ , followed by the further reaction of  $\text{OCIO}$  with NO to produce  $\text{ClO}$ ,  $\text{Cl}$  and  $\text{Cl}_2$  which play an important role in the oxidation of  $\text{Hg}^0$  [3]. On the basis of such observation, we further examined whether the oxidation of  $\text{Hg}^0$  by using  $\text{NaClO}_2(s)$  proceeds well in the presence of  $\text{NO}_x$  and, eventually, we observed that the co-benefit removal of mercury by using  $\text{NaClO}_2(s)$  in the presence of  $\text{NO}_x$  is possible [4]. However, our previous study focused on only the detailed mechanism behind the oxidation of  $\text{Hg}^0$  and used a packed-bed reactor containing  $\text{NaClO}_2(s)$  within  $\text{N}_2$  balance, instead of the flow system of the real flue gas.  $\text{NaClO}_2(s)$  has a form of powder, indicating that the direct injection of  $\text{NaClO}_2(s)$  is more convenient way than the packed  $\text{NaClO}_2(s)$  when we try to control mercury con-

tained within the real flue gas.

To evaluate the performance of  $\text{NaClO}_2(s)$  injection toward mercury control, it is necessary to know the oxidized weight of  $\text{Hg}^0$  by the loaded weight of  $\text{NaClO}_2(s)$ . Besides, the effectiveness of  $\text{NaClO}_2(s)$  in the real flue gas must be examined because the real flue gas contains other gas components such as  $\text{H}_2\text{O}$ ,  $\text{CO}$ ,  $\text{CO}_2$ ,  $\text{NO}_x$ ,  $\text{H}_2\text{O}$ ,  $\text{SO}_2$  and dust. Therefore, for the first time, we conducted the injection of  $\text{NaClO}_2(s)$  to the real flue gas containing other gas components emitted from the iron-ore sintering plant of steel making works with the following objectives: (1) to confirm the possibility of oxidizing  $\text{Hg}^0$  by the injection of  $\text{NaClO}_2(s)$  into the real flue gas, and (2) to evaluate the oxidized weight of  $\text{Hg}^0$  related to the loaded weight of  $\text{NaClO}_2(s)$ .

### EXPERIMENTAL SECTION

#### 1. Description of the Iron-ore Sintering Plant in a Steel-making Company

We installed a tubular flow reactor in an iron-ore sintering plant of steel making works. The function of a sintering plant is to pro-

**Table 1.** Gas conditions of iron-ore sintering plant conducted the injection of  $\text{NaClO}_2(s)$  for the oxidation of  $\text{Hg}^0$

Flow rate	$250 \text{ Nm}^3 \text{ hr}^{-1}$
Reactor temperature	$135^\circ\text{C}$
Baseline $\text{O}_2$ concentration	14-16%
Baseline $\text{NO}$ concentration	180 ppm
Baseline $\text{SO}_2$ concentration	175 ppm
Baseline $\text{CO}_2$ concentration	2.5%
Baseline $\text{CO}$ concentration	5,850 ppm
Baseline $\text{Hg}^0$ concentration	$<10 \mu\text{g Nm}^{-3}$
Baseline particle concentration	$10 \text{ mg Nm}^{-3}$
Inlet $\text{Hg}^0$ concentrations	$50 \mu\text{g Nm}^{-3}$ , $260 \mu\text{g Nm}^{-3}$

<sup>†</sup>To whom correspondence should be addressed.  
E-mail: jydnshin@rist.re.kr

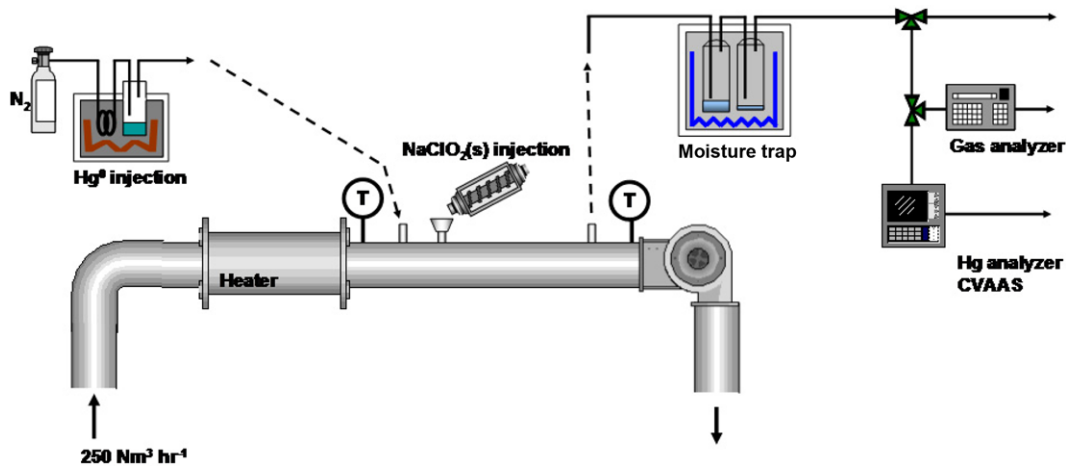


Fig. 1. Schematic diagram of the experimental system.

cess the fine grain of raw iron-ore material into coarse grained iron-ore before being charged to the blast furnace. The flow rate of flue gas emitted from the iron-ore sintering plant is about 1 million  $\text{Nm}^3 \text{ hr}^{-1}$ , where ESP, bag filter and selective catalytic reduction are equipped in series to control the air pollutants. We installed the tubular flow reactor in the duct between ESP and the bag filter. The experimental conditions such as gas composition, temperature and flow rate are listed in Table 1.

## 2. Tubular Flow Reactor and $\text{NaClO}_2(\text{s})$ Injection System

A schematic diagram of the tubular flow reactor is shown in Fig. 1. The flue gas of  $250 \text{ Nm}^3 \text{ hr}^{-1}$  was taken out from the duct of the iron-ore sintering plant by using the induced blower, then introduced into the tubular flow reactor and eventually returned to the duct. The tubular flow reactor was made of steel pipe (10 cm in diameter). The linear velocity of flue gas in the tubular reactor was  $885 \text{ cm s}^{-1}$ . An electric heater was installed between the duct and the tubular flow reactor to control the gas temperature. The temperature difference between two ends of the tubular flow reactor was controlled to be within  $5^\circ\text{C}$ .  $\text{Hg}^0$  was introduced intentionally to the tubular flow reactor by evaporating liquid mercury wrapped by heating tape in which the temperature was controlled. A screw feeder was used to inject  $\text{NaClO}_2(\text{s})$  into the reactor. The photograph of the experi-

mental system used in this study is shown in Fig. 2. The screw feeder supplied  $\text{NaClO}_2(\text{s})$  (density=0.667 g  $\text{cm}^{-3}$ , size=below 0.5 mm) to the reactor at a constant feeding rate, and then the released  $\text{NaClO}_2(\text{s})$  was naturally squeezed into the reactor by the pressure difference between the inside and outside of the tubular flow reactor. The distance between  $\text{NaClO}_2(\text{s})$  and mercury injection ports was separated to 15 cm. The gas sampling port for the analysis of gas composition was 300 cm away from the  $\text{NaClO}_2(\text{s})$  injection port. The inside volume of the tubular flow reactor and the residence time of the flue gas passing between the  $\text{NaClO}_2(\text{s})$  injection and the gas sampling ports were  $23,550 \text{ cm}^3$  and 0.33 s, respectively.

## 3. Gas Analysis and $\text{Hg}^0$ Calibration Procedure

A gas sample of  $10 \text{ L min}^{-1}$  for the analysis of gas composition was taken from the sampling port by using a peristaltic pump. The mercury concentration was determined by using cold vapor atomic absorption spectrometry (CVAAS) having two absorption cells [5]. The concentrations of gas components were monitored with a non-dispersive infrared type of gas analyzer (ZKJ, Fuji Electric Systems Co.). Before the concentrations of gas components were analyzed, the water cooling section for the gas stream was positioned to remove water entering the analyzer.

The mercury analyzer was calibrated with the calibration equipment (Fig. 3). The concentration of  $\text{Hg}^0$  was controlled both by  $\text{N}_2$  flow and by the temperature of the mercury condensation vessels.  $\text{Hg}^0$  was vaporized within a mercury evaporation vessel and swept out by using  $\text{N}_2$  gas passing through the vessel. The  $\text{Hg}^0$  laden  $\text{N}_2$  then entered a saturation vessel within a finely controlled temperature

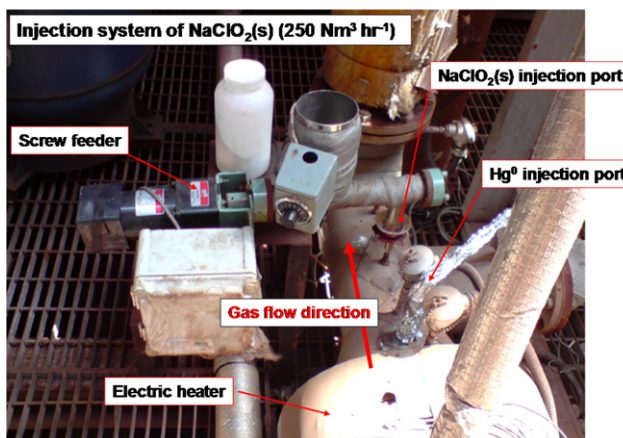


Fig. 2. Photograph of the experimental system.

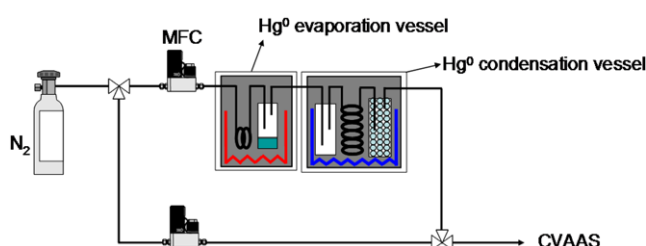
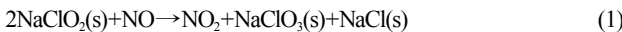


Fig. 3. Schematic diagram of the calibration system for  $\text{Hg}^0$  analyzer. MFC: Mass flow controller.

bath. The gas residence time and surface of condensation materials within the saturation vessel ensured that the gas stream of  $\text{Hg}^0$  in  $\text{N}_2$  was saturated with  $\text{Hg}^0$  vapor at the controlled temperature of the saturation vessel. The temperature of  $\text{Hg}^0$  evaporation vessel was set to ensure that the mercury content of the gas stream leaving the evaporation vessel was greater than that of the saturation concentration corresponding to the value of the saturation vessel temperature. The stream of  $\text{N}_2$  and  $\text{Hg}^0$  exiting the saturation vessel was diluted prior to entering to the CVAAS. In such a way, we obtained the signal of the  $\text{Hg}^0$  concentration by using CVAAS.

## RESULTS AND DISCUSSION

We injected  $\text{NaClO}_2(s)$  into the tubular flow reactor containing  $50 \mu\text{g Nm}^{-3}$  of  $\text{Hg}^0$ , where the feeding rate of  $\text{NaClO}_2(s)$  was set to  $0.06 \text{ g Nm}^{-3}$  (Fig. 4). As soon as  $\text{NaClO}_2(s)$  was introduced into the tubular flow reactor,  $\text{Hg}^0$  was decreased suddenly to  $10 \mu\text{g Nm}^{-3}$ . In our previous study, we observed that the introduced NO reacts with  $\text{NaClO}_2(s)$  to produce  $\text{NO}_2$  through the following reaction:



The generated  $\text{NO}_2$  further reacts with  $\text{NaClO}_2(s)$  to produce  $\text{OCIO}$  through the reaction (2):



$\text{OCIO}$  also can react with NO to give rise to the formation of  $\text{ClO}$ ,  $\text{Cl}$  and  $\text{Cl}_2$  via the reaction channels of (3), (4) and (5) [6],



These chlorine-containing species of  $\text{ClO}$ ,  $\text{Cl}$  and  $\text{Cl}_2$  can significantly oxidize  $\text{Hg}^0$  to  $\text{HgCl}_2$  and  $\text{HgO}$ . However, we did not confirm whether the removed  $\text{Hg}^0$  by injecting  $\text{NaClO}_2(s)$  was exactly  $40 \mu\text{g Nm}^{-3}$  as shown in Fig. 4. When  $\text{SO}_2$  presents with  $\text{Hg}^0$  in flue gas, it can interfere with the detection of  $\text{Hg}^0$ , because it also absorbs the light of  $253.7 \text{ nm}$  used in CVAAS [7]. Typically, solutions con-

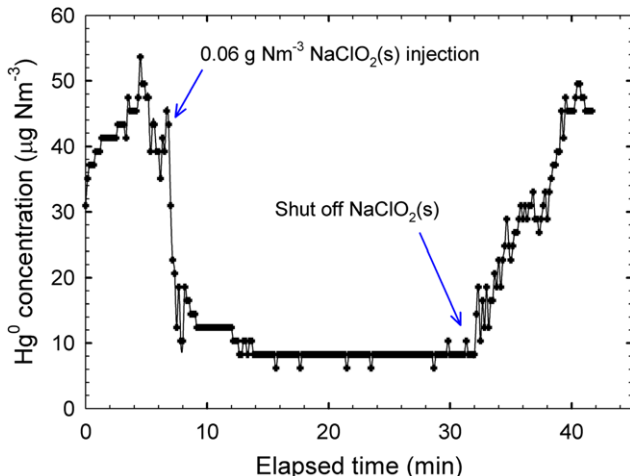


Fig. 4. Temporal profile of  $\text{Hg}^0$  concentration obtained by the injection of  $\text{NaClO}_2(s)$  at  $50 \mu\text{g Nm}^{-3}$  of  $\text{Hg}^0$ .

taining  $\text{NaOH}$  or  $\text{Na}_2\text{CO}_3$  have been used to remove  $\text{SO}_2$  [8]. Solid  $\text{NaOH}$  granules also have been used [9]. Although the flue gas of an iron-ore sintering plant contains about 175 ppm of  $\text{SO}_2$  as listed in Table 1, we did not employ such a system to remove acidic gas of  $\text{SO}_2$ , because  $\text{NaClO}_2(s)$  and  $\text{Cl}_2$  can be dissolved in solutions to result in oxidizing  $\text{Hg}^0$ . The solid  $\text{NaOH}$  granules can also absorb  $\text{Hg}^0$ . Therefore, the  $\text{Hg}^0$  concentration of about  $10 \mu\text{g Nm}^{-3}$  shown in Fig. 4 originates from the signal of  $\text{SO}_2$  contained in the flue gas. Since we cannot overcome such an interference of  $\text{SO}_2$  at the present stage, we have planned to utilize a gold amalgamation method equipped with cold vapor atomic fluorescence spectrometry.

It is difficult to obtain the oxidized weight of  $\text{Hg}^0$  related to the loaded weight of  $\text{NaClO}_2(s)$  in these experimental conditions containing just  $50 \mu\text{g Nm}^{-3}$ , because  $\text{Hg}^0$  is oxidized completely, which indicates that the injected amount of  $\text{NaClO}_2(s)$  is too much as compared to that of  $\text{Hg}^0$  in flue. Under the present experimental conditions, there are two possible methods to obtain the oxidized weight of  $\text{Hg}^0$  related to the loaded weight of  $\text{NaClO}_2(s)$ . One is to increase the concentration of  $\text{Hg}^0$  and the other is to decrease the feeding rate of  $\text{NaClO}_2(s)$ . The minimum feeding rate of  $\text{NaClO}_2(s)$  is  $0.05 \text{ g Nm}^{-3}$  in our screw feeder, implying that decreasing the feeding

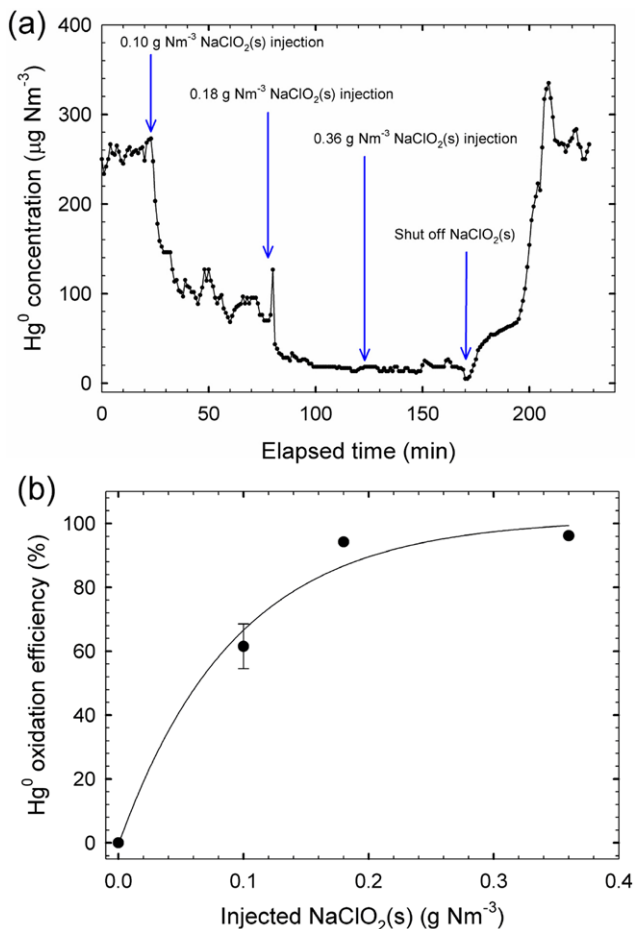
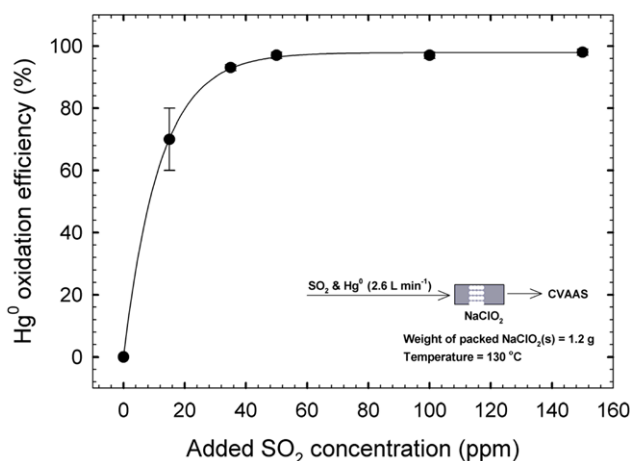


Fig. 5. Oxidation of  $\text{Hg}^0$  by  $\text{NaClO}_2(s)$  injection. (a) Temporal profile of  $\text{Hg}^0$  concentration. (b)  $\text{Hg}^0$  oxidation efficiency as a function of weight of injected  $\text{NaClO}_2(s)$ . Error bars represent the standard deviation of Fig. 5(a) for the measurement duration of about 50 min.

rate is difficult. Therefore, we increased the concentration of  $\text{Hg}^0$  to 260  $\mu\text{g Nm}^{-3}$  (Fig. 5). At first, 0.1 g  $\text{Nm}^{-3}$  of  $\text{NaClO}_2(s)$  was introduced into the tubular flow reactor. The  $\text{Hg}^0$  concentration began to drop suddenly and reached 100  $\mu\text{g Nm}^{-3}$  (Fig. 5(a)). As the injection weight of  $\text{NaClO}_2(s)$  was increased to 0.18 g  $\text{Nm}^{-3}$ , about 90% of  $\text{Hg}^0$  oxidation efficiency was achieved. When the injection weight of  $\text{NaClO}_2(s)$  was further increased to 0.36 g  $\text{Nm}^{-3}$ , the oxidation efficiency of  $\text{Hg}^0$  was achieved to be over 92% (Fig. 5(b)). Based on these experimental results, we obtained the oxidized weight of  $\text{Hg}^0$  related to the loaded weight of  $\text{NaClO}_2(s)$ , i.e., 1026 ( $\pm 333$ ) ( $\mu\text{g-Hg}^0$ ) ( $\text{g-NaClO}_2(s)$ ) $^{-1}$ .

The amount of  $\text{NaClO}_2(s)$ , for example, used in 1 million  $\text{Nm}^3 \text{hr}^{-1}$  is calculated to be about 936 kg day $^{-1}$  (1,403 L day $^{-1}$ ) for 40  $\mu\text{g Nm}^{-3}$  of  $\text{Hg}^0$  oxidation, which was estimated from the oxidized weight of  $\text{Hg}^0$  related to the loaded weight of  $\text{NaClO}_2(s)$ . Based on this observation, we concluded that the simple injection of powdered  $\text{NaClO}_2(s)$  into the flue gas has a potential to achieve over 90%  $\text{Hg}^0$  oxidation in practical application.

The iron-ore sintering flue gas contains many other gas components which can influence the oxidation of  $\text{Hg}^0$ . Therefore, we investigated their effect on the oxidation of  $\text{Hg}^0$  by using a laboratory scale of the experimental system. Since the overall experimental system of laboratory scale was described in detail elsewhere [3], only a general outline of the scheme was inset in Fig. 6. Initially, the effect of  $\text{SO}_2$  on the  $\text{Hg}^0$  oxidation was investigated in this study. 1.2 g of  $\text{NaClO}_2(s)$  was packed within the packed-bed reactor for which the temperature was set to 130 °C and then only  $\text{Hg}^0$  (260  $\mu\text{g Nm}^{-3}$ ) in 2.6 L  $\text{min}^{-1}$   $\text{N}_2$  balance was introduced to the reactor. As shown in Fig. 6, no oxidation of  $\text{Hg}^0$  occurred. As soon as 15 ppm  $\text{SO}_2$  was introduced into the packed-bed reactor,  $\text{Hg}^0$  oxidation occurred suddenly to give about 70% of the oxidation efficiency. With further increase of the addition of  $\text{SO}_2$  to 35 ppm, the complete oxidation of  $\text{Hg}^0$  was obtained. Although the insight into the oxidation mechanisms cannot be verified well presently, this result



**Fig. 6. Effect of  $\text{SO}_2$  on  $\text{Hg}^0$  oxidation by  $\text{NaClO}_2(s)$ .** These data were obtained at the laboratory-scale experiment using packed bed reactor. The inset describes the experiment setup. More detailed experimental system is described in our previous studies [3]. Experimental conditions: total flow rate = 2.6 L  $\text{min}^{-1}$ , temperature = 130 °C, weight of packed  $\text{NaClO}_2(s)$  = 1.2 g,  $\text{N}_2$  balance.

demonstrated that  $\text{SO}_2$  can enhance greatly the oxidation of  $\text{Hg}^0$ . We also investigated the effect of  $\text{H}_2\text{O}$ ,  $\text{CO}$ ,  $\text{CO}_2$  and  $\text{O}_2$  on the  $\text{Hg}^0$  oxidation and observed little enhancement of  $\text{Hg}^0$  oxidation within experimental errors; the concentration of each gas component was increased from 0 to 200 ppm with five loading steps. Upon the basis of these results, we concluded that the most important species influencing the oxidation of  $\text{Hg}^0$  is  $\text{SO}_2$ , rather than  $\text{H}_2\text{O}$ ,  $\text{CO}$ ,  $\text{CO}_2$  and  $\text{O}_2$ .

As can be seen in Figs. 4 and 5(a), the concentration of  $\text{Hg}^0$  was increased when the injection of  $\text{NaClO}_2(s)$  was stopped. However, the time for the  $\text{Hg}^0$  concentration to reach the initial value of  $\text{Hg}^0$  concentration took about 30 min. Considering the residence time of the flue gas passing the reactor (0.33 s), the accumulated  $\text{NaClO}_2(s)$  on the inner surface of the reactor has caused the slow increase of  $\text{Hg}^0$  concentration. Although we did not use the particulate control equipment in the present stage, it must be used in the case of a larger system than the present one to prevent the release of the  $\text{NaClO}_2(s)$  into the atmosphere. A bag house as a particulate control equipment can provide better interaction between gas and  $\text{NaClO}_2(s)$  due to the accumulation of the  $\text{NaClO}_2(s)$  on the surface of the bag house. If so, installing a bag house gives rise to reducing the amount of  $\text{NaClO}_2(s)$ , which is necessary to oxide  $\text{Hg}^0$ . Therefore, we feel that further studies by employing a bag house are essential to extract the required weight of  $\text{NaClO}_2(s)$  in a practical application.

## CONCLUSIONS

Effects of the  $\text{NaClO}_2(s)$  injection on the oxidation of  $\text{Hg}^0$  were evaluated experimentally in a bench scale tubular flow reactor where the flue gas emitted from iron-ore sintering plant of steel making works is used. This study demonstrated that the direct injection of  $\text{NaClO}_2(s)$  within flue gas can be applicable for  $\text{Hg}^0$  emission control for a practical application. In addition, we feel that, as a next step, a long-term reliable test of this process using a bag house at a low  $\text{Hg}^0$  concentration (below 50  $\mu\text{g Nm}^{-3}$ ) is necessary. The following conclusions were obtained by this study:

(1)  $\text{Hg}^0$  oxidation efficiency of 90% was obtained at the feeding rate of 0.18 g  $\text{Nm}^{-3}$   $\text{NaClO}_2(s)$ , which corresponds to the oxidized weight of  $\text{Hg}^0$  related to the loaded weight of  $\text{NaClO}_2(s)$  being 1026 ( $\pm 333$ ) ( $\mu\text{g-Hg}^0$ ) ( $\text{g-NaClO}_2(s)$ ) $^{-1}$ ;

(2)  $\text{SO}_2$  species contained in flue gas accelerated the oxidation of  $\text{Hg}^0$ , whereas  $\text{CO}$ ,  $\text{CO}_2$ ,  $\text{H}_2\text{O}$  and  $\text{O}_2$  had little effect on the  $\text{Hg}^0$  oxidation;

(3) The accumulated  $\text{NaClO}_2(s)$  inside the tubular reactor enhanced the oxidation of  $\text{Hg}^0$ , implying that installing a bag house will reduce the required amount of the  $\text{NaClO}_2(s)$  injection for  $\text{Hg}^0$  oxidation.

## ACKNOWLEDGEMENTS

This work was supported by the Power Generation & Electricity Delivery (20091020100080) of the Korea Institute of Energy Technology Evaluation and Planning (KETEP) grant funded by the Korea government Ministry of Knowledge Economy.

## REFERENCES

1. W. H. Schroeder and J. Munthe, *Atmos. Environ.*, **32**, 809 (1998).

Korean J. Chem. Eng.(Vol. 28, No. 3)

2. J. M. Pavlish, E. V. Sondreal, M. D. Mann, E. S. Olson, K. C. Galbreath, D. L. Laudal and S. A. Benson, *Fuel Process. Technol.*, **82**, 89 (2003).
3. Y. Byun, K. B. Ko, M. Cho, W. Namkung, K. Lee, D. N. Shin and D. J. Koh, *Environ. Sci. Technol.*, **43**, 5054 (2009).
4. Y. Byun, K. B. Ko, M. Cho, W. Namkung, D. J. Koh, K. Lee, I. P. Hamilton and D. N. Shin, *Environ. Sci. Technol.*, **44**, 1624 (2010).
5. Y. Byun, K. B. Ko, M. Cho, W. Namkung, D. N. Shin, J. W. Lee, D. J. Koh and K. T. Kim, *Chemosphere*, **71**, 1674 (2008).
6. Z. Li, R. D. Wuebbles and N. J. Pylawka, *Chem. Phys. Lett.*, **354**, 491 (2002).
7. H. Okabe, *Photochemistry of small molecules*, John Wiley & Sons, New York (1978).
8. H. K. Choi, S. H. Lee and S. S. Kim, *Fuel Process. Technol.*, **90**, 107 (2009).
9. S. Straube, T. Hahn and H. Koeser, *Appl. Catal. B*, **79**, 286 (2008).